Journal of Research and Applications in Mechanical Engineering
ISSN: 2229-2152 (Print); 2697-424x (Online)
(2025) Vol. 13, No. 2, Paper No. JRAME 25-13-027
[DOI: 10.14456/jrame.2025.27]

Research Article

Numerical Investigation of the Greenhouse with the Floor and Other Cooling Systems

U. Srangtham [1]
A. Pramuanjaroenkij[2]
P. Janthasri[1]
S. Dokkaew[1]
S. Kakac[3]
A. Tongkratoke[1,*]
[1] *Department of Mechanical and Manufacturing Engineering, Faculty of Science and Engineering, Kasetsart University, Chalermphrakiat Sakon Nakhon Province Campus, Sakon Nakhon, 47000 Thailand*
[2] *Kasetsart University International College, Bangkok, 10903 Thailand*
[3] *Department of Mechanical Engineering, TOBB University of Economics and Technology, Ankara, 06560 Turkey*

Received 18 September 2024
Revised 21 November 2024
Accepted 26 November 2024

Abstract:
This study used computational fluid dynamics (CFD) simulations to explore the effect of the greenhouse with the floor and other cooling systems (only an evaporative cooling system, only a floor cooling system, and equipped with both cooling systems) on temperature distributions inside a greenhouse. Three scenarios were analyzed using the finite volume method and several the Realizable k-ε turbulence model offered superior accuracy compared to the Standard k-ε model in simulating temperature distributions. However, significant discrepancies were observed near the wall surfaces of the greenhouse. To address this, a radiation model was incorporated alongside the Realizable k-ε turbulence model, which improved simulation accuracy by reducing error percentages down to 2-3% and better matching experimental results. The study emphasizes the importance of using the Realizable k-ε turbulence model with the radiation model to improve the accuracy of CFD simulations for the greenhouse with the floor and other cooling systems.

Keywords: *Turbulence model, Computational Fluid Dynamics, Radiation floor cooling system, Heat Transfer*

1. Introduction

With the rapid evolution of engineering techniques in material, agricultural, and building industry, HVAC (heating, ventilation, and air conditioning) systems, and greenhouse are integrated, especially, evaporative cooling systems are widely utilized in many countries to save energy, improve comfort, and promote health. Radiant floor heating and cooling technology is a system that regulates the temperature of a space by utilizing the floor as a large thermal mass. To provide cooling, it works by pumping cool water through floor-mounted pipes. This approach is especially successful for cooling greenhouses in locations with ambient temperatures above 40°C [1] and performs better in areas with low ambient relative humidity [2].

Many researchers have attempted to improve the effectiveness of floor cooling systems by applying computational fluid dynamics (CFD) to analyze various issues; floor cooling, evaporative cooling, and radiation in the greenhouse. Wu et al. [3] created a simple model utilizing a conduction form factor, allowing the heat transfer and surface temperature of cooling or radiant floor systems to be computed. It was noticed that the thickness of the screed had a minimal effect on thermal resistance, while the spacing of the pipes and the average water temperature significantly influenced it.

In order to study the system for various climate zones in India, Srivastava et al. [4] combined an evaporative cooling system with a radiant cooling system. In this study, two primary systems were analyzed: the chiller and cooling tower

* Corresponding author: A. Tongkratoke
E-mail address: ammarin.to@ku.th

operated by the radiant cooling system. The radiant cooling system operated by water provided an annual savings of 7% in hot and dry climates via the cooling tower, as well as 11% annual savings in composite climates.

Zheng et al. [5] developed a three-dimensional heat transfer model for a radiant floor system to analyze the impact of non-heating surface temperature on heat output and computing the floor surface temperature using the CFD approach. Regardless of how accurate the three-dimensional model for radiant floor systems was, calibrating the model's physics increased the computational burden [6].

The study by Dong et al. [7] uses numerical simulations to assess the heating effectiveness of a radiant-convective heating terminal. The objective is to understand how the combined radiant and convective heating mechanisms impact temperature distribution and thermal comfort within a space, with a goal on providing uniform heating. This involves examining temperature profiles, heat distribution, and overall system efficiency under various operational conditions. The study utilizes advanced CFD tools to model the heating terminal's performance. The simulation incorporates both radiant and convective heat transfer mechanisms.

Micko et al. [8] conducted an experimental study to verify the accuracy of CFD simulations in predicting the operative temperature (OT) and mean radiant temperature (MRT) in indoor environments heated by radiator and floor heating systems. The study compares simulation results with experimental measurements obtained in a controlled room setup. The findings demonstrate the effectiveness of CFD models in predicting thermal comfort parameters, highlighting both the strengths and limitations of the simulation approach.

Liu et al. [9] presented a novel approach for estimating the radiant floor cooling system's cooling capability by developing a simplified numerical calculation method coupled with the Back Propagation (BP) neural network model. The goal was to create a reliable and efficient tool for predicting the cooling performance of such systems under various operating conditions, allowing for better design and optimization. The simplified numerical model and BP neural network provided results comparable to those from detailed CFD simulations but with significantly reduced computational time and resources.

Moreover, the utilization of thermal mass in the radiant floor system necessitates transient simulation to accurately depict system performance. From this perspective, to assess the impact of certain greenhouse building components, including ventilation rates and temperature conditions, an alternative numerical method can be utilized [10].

This work uses comprehensive Computational Fluid Dynamics (CFD) simulations to compare various cooling arrangements in detail for greenhouse temperature management: Case 1, with only an evaporative cooling system; Case 2, with only a floor cooling system; and Case 3, equipped with both a floor cooling system and an evaporative cooling system. Few studies have used CFD simulations to analyze evaporative cooled greenhouse, comparing results with experimental data from greenhouse studies [11]. Hence, validated turbulence models (Standard k-ε and Realizable k-ε) and radiation model to increase simulation accuracy, especially in the vicinity of the greenhouse walls and operational parameters, including temperature distribution and ventilation rates. In practical greenhouse applications, this method helps to optimize cooling system designs and offers a more accurate prediction of temperature and velocity profiles.

2. Methodology

The radiant floor cooling system's performance was evaluated using a three-dimensional greenhouse model. Boundary conditions were introduced with the numerical technique. Computational Fluid Dynamics validations were finally conducted via comparisons with the experiment data (Figure 1) of Nuyjanthuek and Pramuanjaroenkij [11].

2.1 The physical model

In this investigation, as seen in Figure 2, a three-dimensional greenhouse model was suggested that included other cooling systems in addition to the radiant floor cooling system. This schematic represented the typical air-conditioned room with a no-cooling floor, the system of evaporative cooling, and radiant floor cooling. The three dimensions of the greenhouse model were 3.3 x 2.2 x 1.9 meters in length, width, and height. An evaporative cooling system was used in the greenhouse, consisting of an evaporative pad (width 0.9 meters x height 1.4 meters) and two exhaust fans (0.5 kW, 220V) located at the opposite end of the greenhouse.

Fig. 1. The greenhouse configuration of Nuyjanthuek and Pramuanjaroenkij [11]

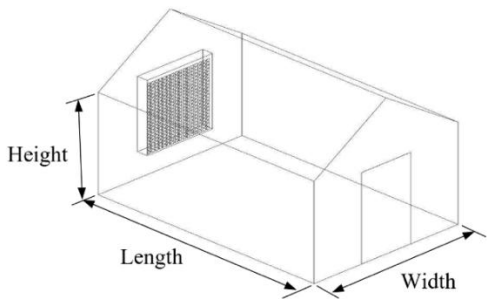

Fig. 2. Schematic of the three-dimensional greenhouse

Figures 3, 4, and 5 presented the CFD geometric representation of the greenhouse under three different cooling setups: only an evaporative cooling system, only a floor cooling system, and a combination of both systems, respectively. All boundary conditions and the CFD model's parameters were detailed in Table 1.

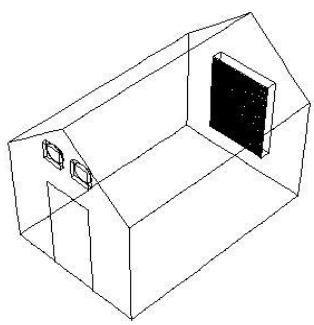

Fig. 3. CFD geometric model for the first case: the greenhouse with only the evaporative cooling system

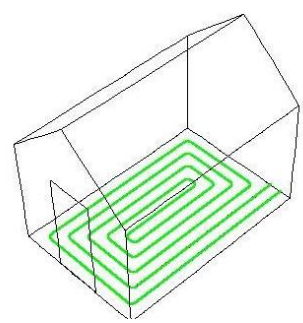

Fig. 4. CFD geometric model for greenhouse with only floor cooling system (case 2)

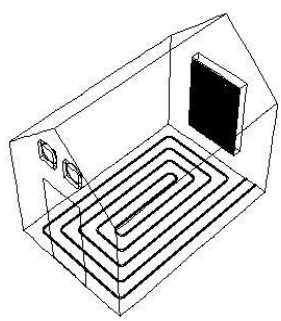

Fig. 5. CFD geometric model for a greenhouse with both a floor cooling system and an evaporative cooling system (case 3).

Table 1: The greenhouse model's boundary conditions and parameters.

Properties	Value/Unit	
Air density	1.225	kg/m^3
Thermal conductivity coefficient	0.0225	W/m K
Specific heat	1.005	kJ/kg K
Viscosity	1.83×10^{-5}	kg/m s
Glass density	2500	kg/m^3
Thermal conductivity coefficient	0.74	W/m.K
Heat transfer coefficient	6.4	W/m^2 K
Inlet velocity	0.8	m/s
Outlet velocity	6.0	m/s
Outside radiation	660	W/m^2
Ambient temperature	33	^oC

2.2 The mathematical model

The finite volume method was used to conduct the numerical simulations [12]. The continuity, momentum, and energy equations were resolved using the k-epsilon (k-ε) turbulence model [13], while the momentum equation near the region of wall surfaces and the flow fields in the outside region was computed using the Realizable k-ε turbulence model [14].

Continuity equation

$$\frac{\partial}{\partial x_i}(\rho u_i) = 0 \tag{1}$$

Momentum equation

$$\frac{\partial}{\partial x_j}(\rho u_i u_j) + \frac{\partial \rho u_i}{\partial x_i} = \frac{\partial}{\partial x_j}\left\{\mu\left(\frac{\partial u_i}{\partial x_j} + \frac{\partial u_j}{\partial x_i}\right)\right\} - \frac{\partial P}{\partial x_i} - \frac{\partial \rho \overline{u}_i \overline{u}_j}{\partial x_j} + \rho g_i \tag{2}$$

Energy equation

$$\frac{\partial}{\partial x_j}(\rho u_j T) = \frac{\partial}{\partial x_j}\left[\left(\frac{\mu}{\Pr} + \frac{\mu_t}{\sigma_t}\right)\frac{\partial T}{\partial x_j}\right] + S_T \tag{3}$$

The Reynolds-averaged Navier-Stokes (RANS) turbulence models can be divided into two groups: Reynolds stress models (RSMs) and Eddy viscosity models (EVMs). The EVMs are based on the Bossiness' theory [15], where the Reynolds stress with respect to the strain rate is given by:

$$-\frac{\partial \rho \overline{u}_i \overline{u}_j}{\partial x_j} = \mu_t\left(\frac{\partial u_i}{\partial x_j} + \frac{\partial u_j}{\partial x_i}\right) - \frac{2}{3}\delta_{ij}\rho k \tag{4}$$

Where $k = \frac{1}{2}u_i u_j$ is the turbulent kinetic energy, μ_t is a model eddy viscosity, and δ_{ij} is the Kronecker delta ($\delta_{ij} = 1$ if $i = j$ and $\delta_{ij} = 1$ if $i \neq j$). Substituting the equation (4) into equation (2) the momentum equation can be revised as:

$$\frac{\partial}{\partial x_i}(\rho u_i k) = \frac{\partial}{\partial x_j}\left[\left(\frac{\mu_t}{\sigma_k} + \mu\right)\frac{\partial k}{\partial x_i}\right] + \rho\varepsilon - G_k \tag{5}$$

$$\frac{\partial}{\partial x_i}(\rho u_i \varepsilon) = \frac{\partial}{\partial x_j}\left[\left(\frac{\mu_t}{\sigma_\varepsilon} + \mu\right)\frac{\partial \varepsilon}{\partial x_i}\right] + \rho C_1 \varepsilon S - \rho C_2 \frac{\varepsilon^2}{\sqrt{\nu\varepsilon} + k} \tag{6}$$

$$C_1 = \max\left[0.43, \frac{\eta}{5+\eta}\right] \tag{7}$$

$$\eta = kS/\varepsilon \tag{8}$$

$$S = \sqrt{2S_{ij}S_{ij}} \tag{9}$$

$$S_{ij} = \frac{1}{2}\left(\frac{\partial u_i}{\partial x_j} + \frac{\partial u_j}{\partial x_i}\right) \tag{10}$$

The Realizable k-ε turbulence model is represented by equations (5) through (10). The Realizable k-ε turbulence model's eddy viscosity can be expressed as follows:

$$\mu_t = \rho C_\mu \frac{k^2}{\varepsilon} \tag{11}$$

$$C_\mu = \frac{1}{A_0 + A_s \frac{k}{\varepsilon} U^*} \tag{12}$$

$$A_s = \sqrt{6}\cos\varphi \tag{13}$$

$$\varphi = \frac{1}{3}\cos^{-1}(\sqrt{6}W) \tag{14}$$

$$W = S_{ij} \tag{15}$$

Table 2: The model constants used for the Realizable k-ε turbulence model.

A_0	σ_ε	σ_k	$C_{\varepsilon 1}$	C_2
4.04	1.20	1.00	1.44	1.90

Launder and Spalding [16] proposed the standard wall function, with the mean velocity in the y^+ range of 30 to 60. The relationship between the mean velocity and location can be thought of as linear when y^+ is less than thirty. The mean velocity law of the wall can be written as

$$U^* = \frac{1}{\kappa}\ln\left(y^* E\right) \tag{16}$$

$$y^* = \frac{\rho C_\mu^{1/4} k^{1/2} y}{\mu} \tag{17}$$

$$y^+ = \frac{\rho u_\tau y}{\mu} \tag{18}$$

The variables κ, E, μ_τ and y represent the Kármán constant (equals to 9.793), constant of empirical (equals to 9.793), friction velocity, and the distance from a point to the wall, respectively.

Radiative energy source term or Radiation model

For equations (3), S_T is defined as equations (19)

$$S_T = a(4\hat{\sigma}T^4 - \overline{G}) \tag{19}$$

In this case, the constant of Stefen-Boltzmann is $\hat{\sigma}$, the absorption coefficient is a, and the obtained for radiative transfer is $\overline{G}$, which is defined as

$$\frac{dI(\vec{r},\vec{s})}{ds} + (\sigma_s + a)I(\vec{r},\vec{s}) = \frac{\sigma T^4}{\pi} an^2 + \frac{\sigma_s}{4\pi}\int_0^{4\pi} \Phi(\vec{s},\vec{s})I(\vec{r},\vec{s})d\Omega' \tag{20}$$

where $\vec{r}$ and $\vec{s}$ are the position and direction of vector, respectively. Ω' and Φ are solid and phase angle, respectively. In addition, n, I, a, and σ_s are refractive index, radiative intensity, absorption coefficient, scattering coefficient, respectively.

2.3 Grid-independent and numerical method

The model was meshed utilizing tetrahedral T-grid elements since they suited better for complex geometry than hexahedral elements. The meshing of the model was done with a grid spacing of 0.03. The Standard and Realizable k-ε turbulence models used approximately 500,542 and 511,431 grid cells, respectively. The mesh size was also tested for grid independence (see Figure 6). The flow domain was solved using the k-ε turbulence model, with the second-order upwind approach for discretization. The flow velocity and pressure were coupled using the semi-implicit pressure linkage approach. All simulation cases were iterated until they reached the convergence level of 10^{-6}.

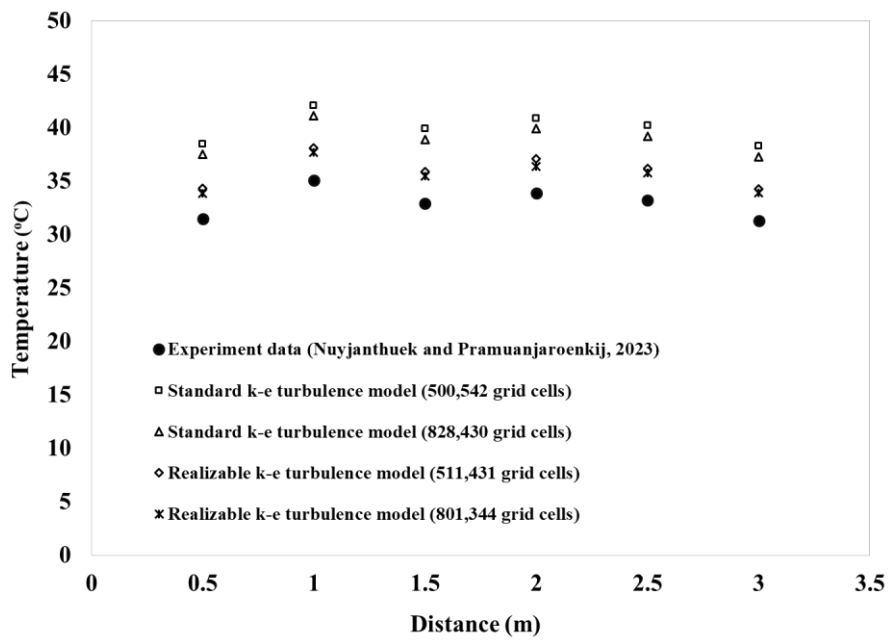

Fig. 6. A comparison of the simulated results outcomes derived from Realizable and Standard k-ε turbulence models and the experiment data of Thanakorn Nuyjanthuek [11] including the grid independence evaluation.

3. Results and Discussions

3.1 Validation of the CFD simulation

The temperatures measurement in the numerical simulation and experiment data [11] obtained from points 1, 2, 3, 4, 5 and 6 (Figure 7); at lengths of 0.5, 1, 1.5, 2, 2.5 and 3 meters, respectively, were compared with the temperature results of the validated simulation was performed using temperature measurements from three scenarios: Case 1 (the greenhouse with only the evaporative cooling system), Case 2 (the greenhouse with only the floor cooling system), and Case 3 (the greenhouse equipped with the evaporative and floor cooling system).

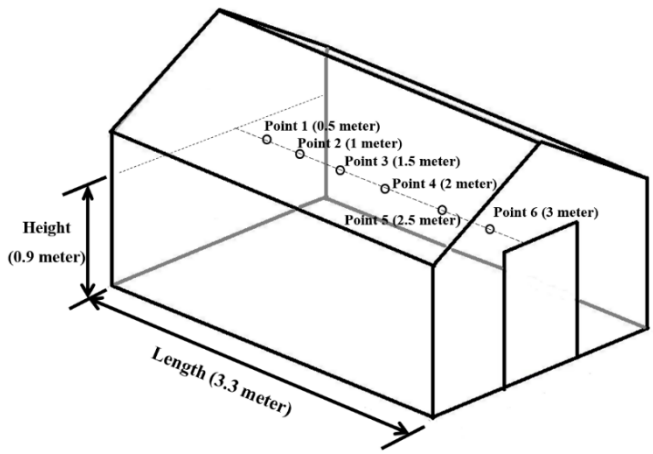

Fig. 7. Temperature measurement points in the numerical simulation and experiment data [11].

The k-ε turbulence model (Figure 8) was simulated for case 1 (Figure 3) and compared with the experiment data of Nuyjanthuek and Pramuanjaroenkij [11]. It was found that this Standard k-ε turbulence model had percentage errors in temperature simulation at the lengths of 0.5, 1, 1.5, 2, 2.5, and 3 meters of 19.05%, 17.09%, 18.24%, 17.70%, 18.07%, and 19.17%, respectively. Also, the numerically simulated results (Realizable k-ε turbulence model) at the lengths of 0.5, 1, 1.5, 2, 2.5, and 3 meters had percentage errors that are 9.05%, 8.55%, 9.12%, 9.44%, 9.04%, and 9.58%, respectively (Figure 8).

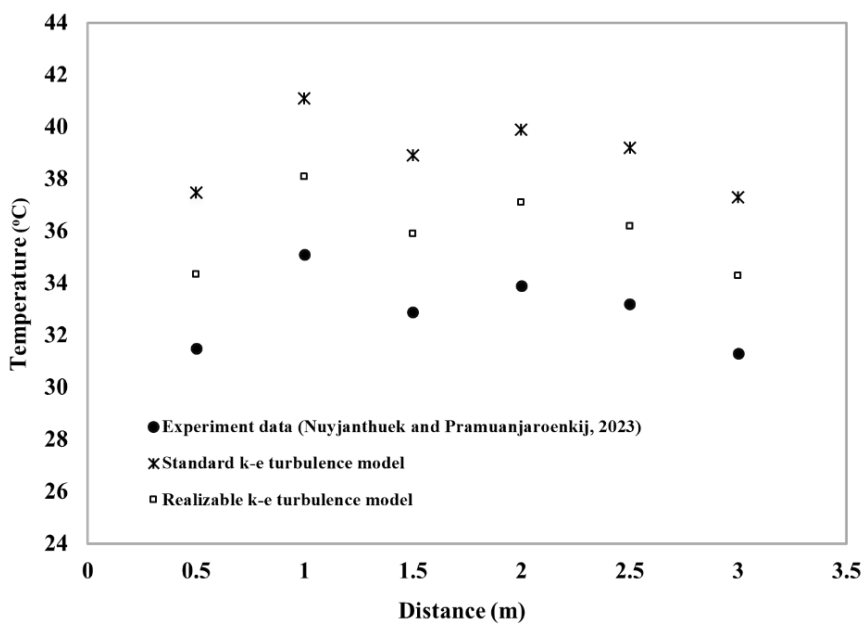

Fig. 8. k-ε turbulence model validation for case 1.

The validation of the k-ε turbulence models for case 2 is displayed in Figure 9. (the greenhouse with only the floor cooling system) against the experiment data from Nuyjanthuek and Pramuanjaroenkij [11]. In case 2, the Standard of k-ε turbulent model, the percentage errors in temperature simulation at lengths of 0.5, 1, 1.5, 2, 2.5 and 3 meters were 18.67%, 10.82%, 12.31%, 12.53%, 12.13% and 12.34% respectively, compared to the experimental data. In addition percentage errors for the numerically simulated results (Realizable k-ε turbulence model) at the same lengths were 9.87%, 6.97%, 8.29%, 8.35%, 8.42% and 9.71%, respectively.

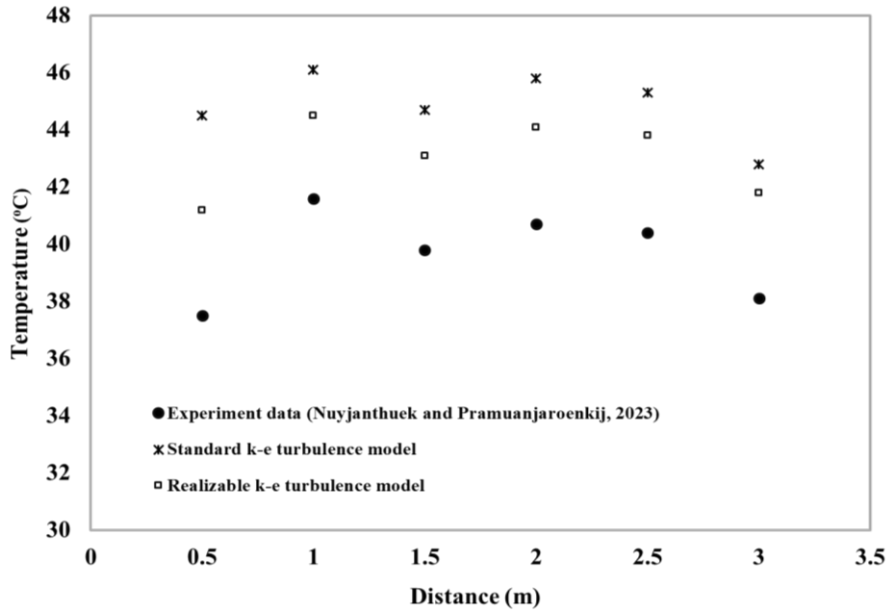

Fig. 9. Validation of k-ε turbulence models for case 2

In case 3, which involves a greenhouse equipped with both floor and evaporative cooling system, the performance of the Realizable and Standard of k-ε turbulence models was evaluated against experimental data from Nuyjanthuek and Pramuanjaroenkij [11]. The validation is illustrated in Figure 10. The Standard of k-ε turbulence model showed percentage errors in temperature simulation that varied significantly with lengths, ranging from 9.14% to 10.16%. For the Realizable of k-ε turbulence models, the percentage errors ranged from 6.57% to 7.42% across lengths from 0.5 to 3 meters, compared to the experimental data.

According to these findings, the Realizable of k-ε turbulence model offers a more accurate representation of temperature distribution in the greenhouse with the floor cooling system, compared to the Standard of k-ε model. The lower errors observed with the Realizable of k-ε model indicate its superior performance in simulating the effects within the floor cooling system.

Compared to the whole performance, the Realizable of k-ε turbulence model exhibited higher percentage errors compared to experimental data at specific heights. Specifically, at lengths of 0.5 and 3 meters, the percentage errors from the Realizable k-ε model were notably higher than those observed in the experimental data provided by Nuyjanthuek and Pramuanjaroenkij [11].

To address these discrepancies and improve the accuracy of the numerical simulations, the researchers incorporated a radiation model alongside the Realizable of k-ε turbulence model. This combination aimed to better account for the temperature effects near the wall surface of a greenhouse, which were not fully captured by the turbulence model alone.

Figure 11 shows a comparison of the temperatures of the Realizable of k-ε turbulence model with the radiation model and the experimental data [11]. The finding is in line with the experimental data. At various lengths of 0.5 and 3 meters, the Realizable of k-ε turbulence model with radiation model gave better numerical simulated results compared to the Realizable of k-ε turbulence model alone, and its results were closest to the model (see Figure 11 (a), (b) and (c)).

Overall, the inclusion of the Realizable of k-ε turbulence model with the radiation model enhances the simulation's performance, particularly at lower lengths (0.5 and 3 meters) where initial errors were more pronounced. This approach effectively reduces the percentage of errors and provides a more accurate representation of the greenhouse environment.

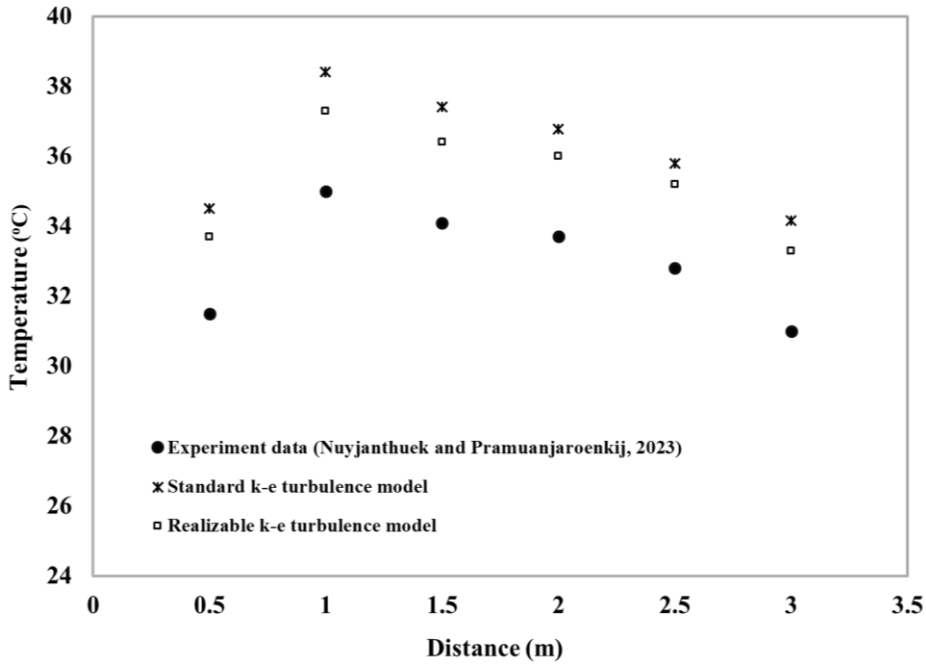

Fig. 10. Validation of k-ε turbulence models for case 3

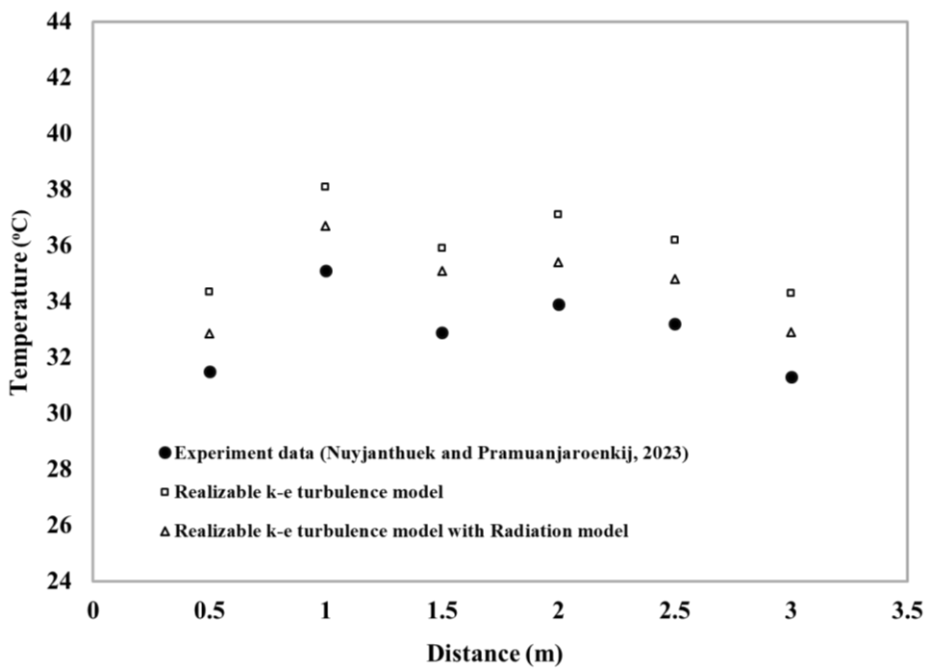

(a)

Fig. 11. Variations in temperatures of the greenhouse for (a) case 1, (b) case 2 and (c) case 3

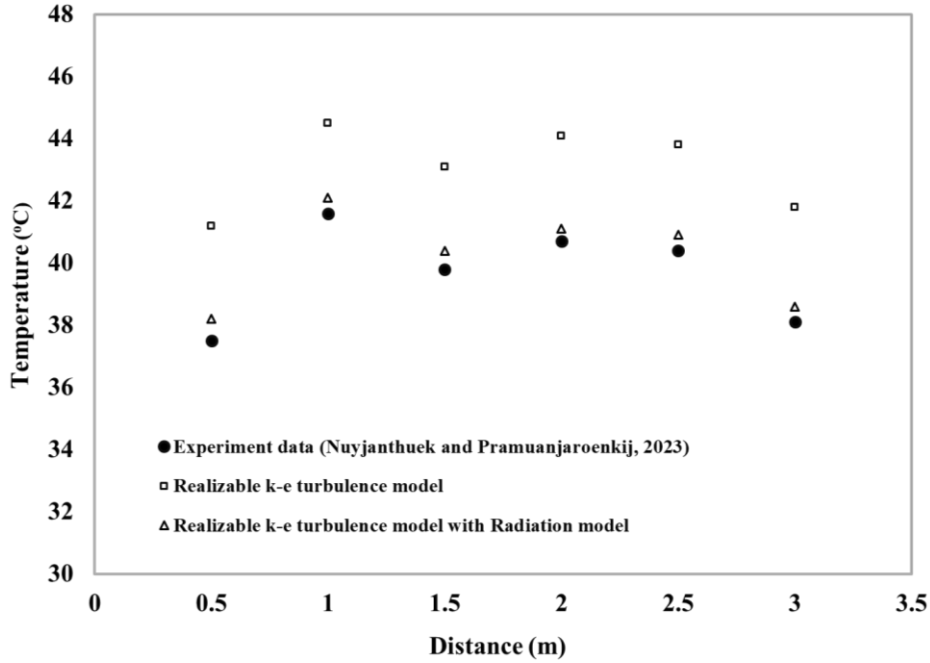

(b)

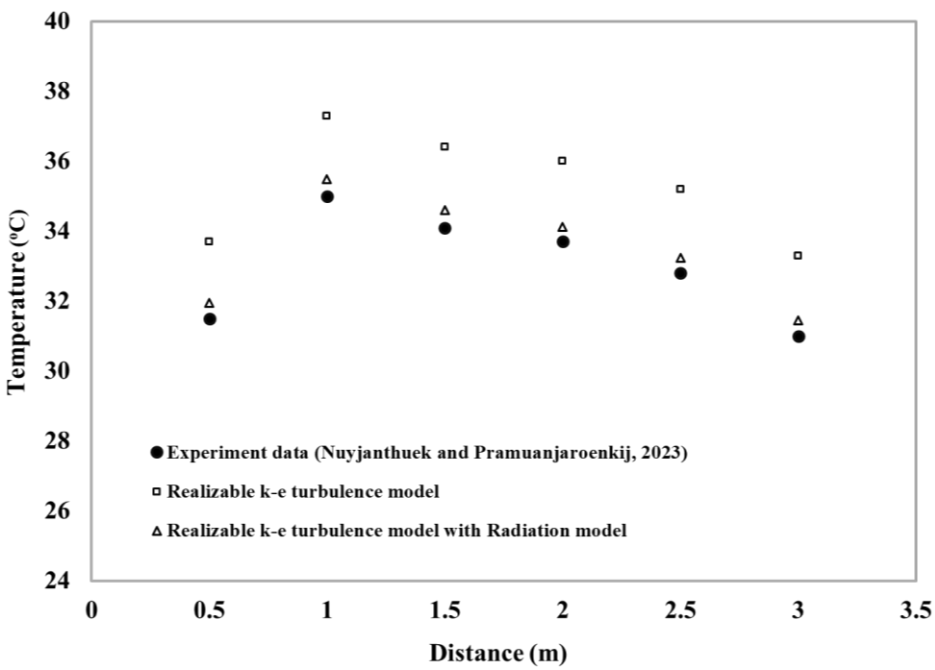

(c)

Fig. 11. (continuous) Variations in temperatures of the greenhouse for (a) case 1, (b) case 2 and (c) case 3

3.2 The air velocity and temperature distribution of the greenhouse with only the evaporative cooling system (Case 1)

The air velocity distribution for case 1 in Figure 12 (a) and (b) indicates that the air velocity inside the greenhouse with only the evaporative cooling system ranges between 0 and 0.07 m/s. The lowest velocity will be at the

greenhouse's surface and walls. Additionally, the air velocity near the evaporative cooling system is 0.11 m/s, which is higher than the air velocity inside the greenhouse.

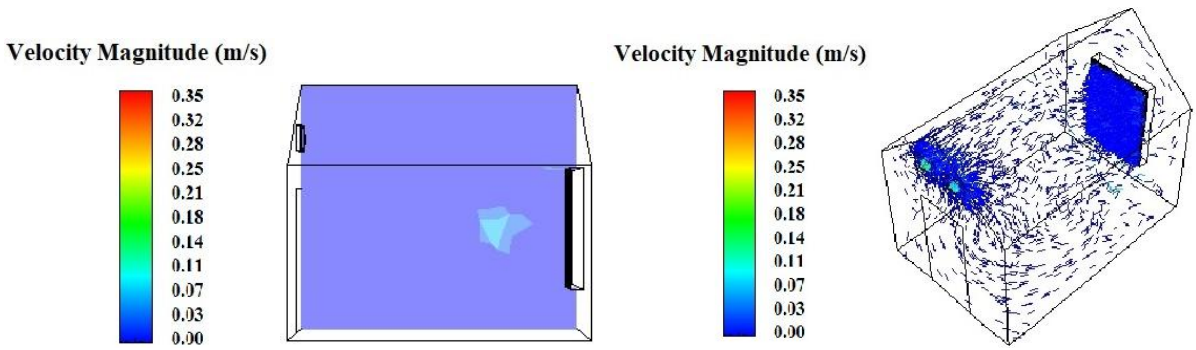

(a) (b)

Fig. 12. The air velocity distribution at the greenhouse's walls and floor (case 1)

The floor and walls of the greenhouse's temperature distribution contours are depicted in Figure 13. A remarkable temperature around the greenhouse with a maximum temperature magnitude of approximately 35 ºC and a minimum temperature magnitude of approximately 25 ºC was observed.

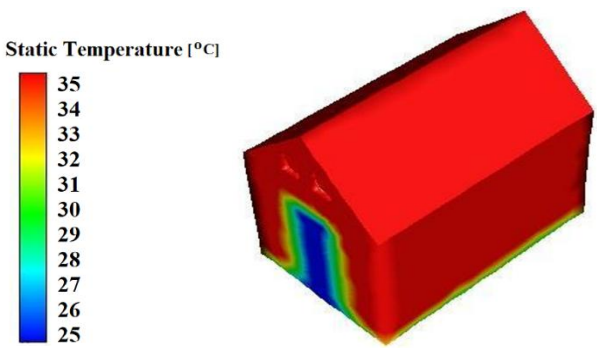

Fig. 13. The distribution of temperatures at the greenhouse's walls and floor (case 1)

The temperature distribution inside the greenhouse for various patterns is shown in Figure 14. The temperature distribution may be clearly understood in relation to the colors. The blue color indicates the low temperature field, while the red color represents the high-temperature field. It can be observed that the floor temperature is cooler compared to the warmer, red-gradient walls (see Figure 14 (a) and (b)). From the simulated data for the greenhouse, we found the average temperature to range from 26.5 ºC to 32.5 ºC at measuring heights of 0.5 to 1.9 meters.

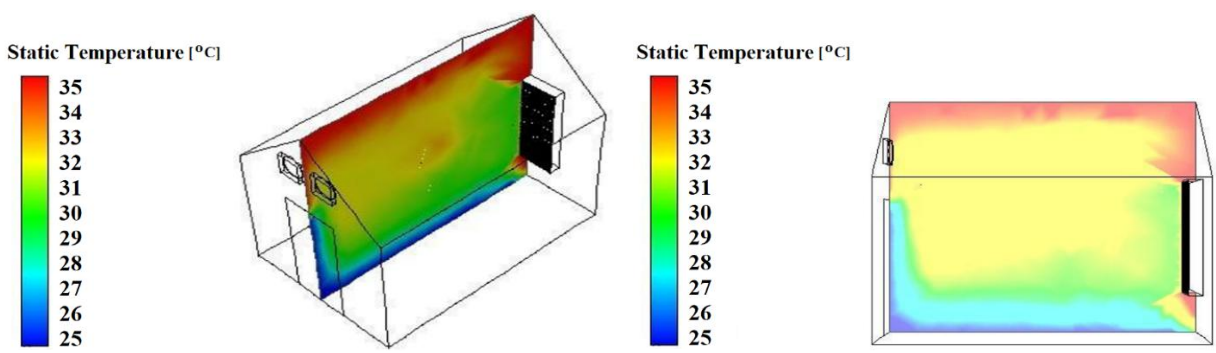

(a) (b)

Fig. 14. The temperature distribution contours at the height measurement (X-Y plane) of 0.5 to 1.9 meters (case 1)

3.3 The air velocity and temperature distribution of the greenhouse with only the floor cooling system (Case 2)

As shown in Figures 15 (a) and (b), the distribution of air velocity inside the greenhouse for Case 2 demonstrates significantly different air flow inside the greenhouse. At a height of 0.8 to 1.1 meters with an air velocity of 1.62 to 1.85 m/s, the center of the greenhouse room has the highest air velocity. The primary system responsible for air movement is the convection cooling system, which produces forced convection of air.

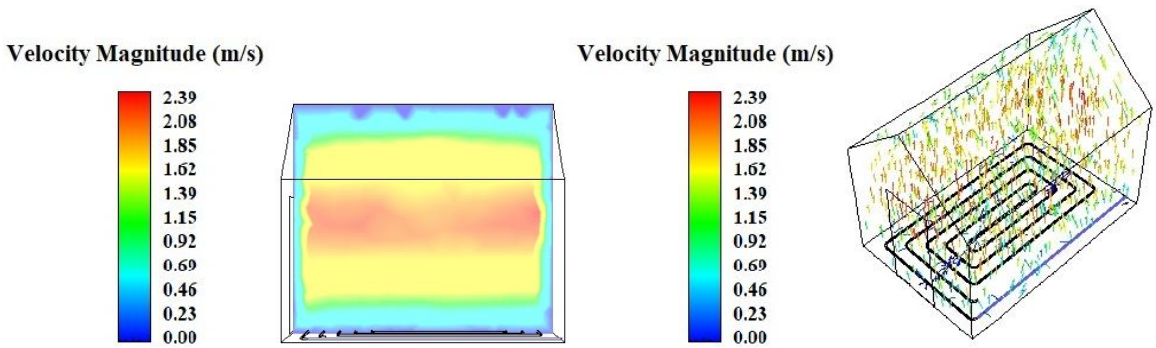

(a) (b)

Fig. 15. The air velocity distribution at the greenhouse's walls and floor (case 2)

The effect of the floor cooling system is illustrated in Figure 16. The system operates with a floor temperature of 21 ºC for air circulation and ventilation within the greenhouse. The figure shows that the maximum and minimum temperatures observed were 37 ºC and 21 ºC, respectively**.**

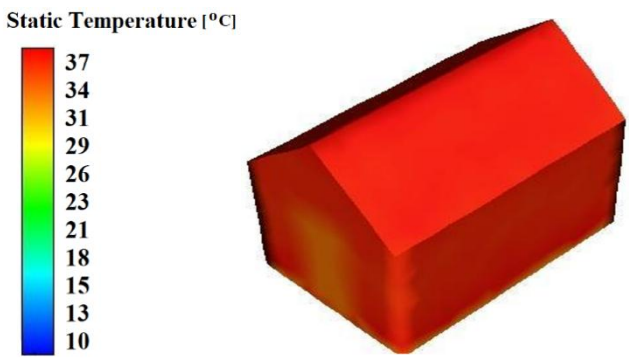

Fig. 16. The distribution of temperatures at the greenhouse's walls and floor (case 2)

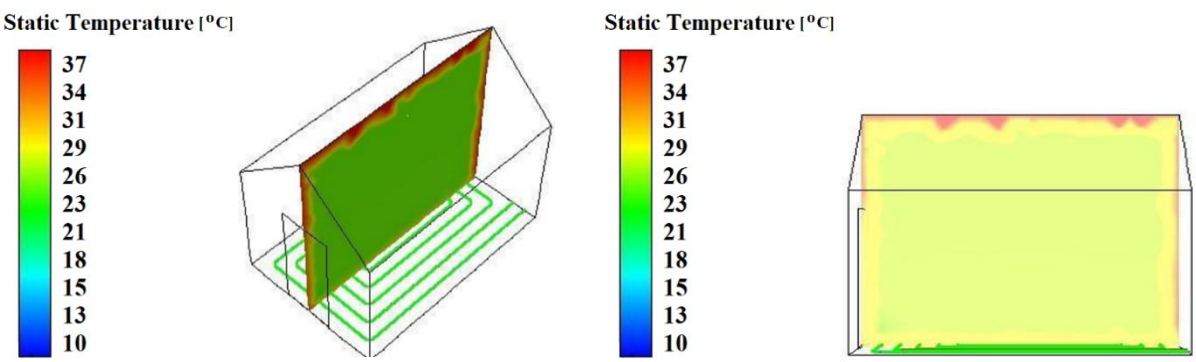

(a) (b)

Fig. 17. The temperature distribution contours at the height measurement (X-Y plane) of 0.5 to 1.9 meters (case 2)

Figures 17 (a) and (b) show temperature distribution simulation results for the greenhouse is outfitted with a floor cooling system in combination. The temperature observed at heights of 0.5, 1.0, 1.5, and 1.9 meters were 21 ºC, 26 ºC, 29 ºC, and 31 ºC, respectively. These results indicate that the integrated floor cooling system effectively lowers and maintains constant indoor temperature.

3.4 The air velocity and temperature distribution of the greenhouse equipped with the evaporative and floor cooling systems (Case 3)

The air velocity distribution of the greenhouse equipped with the evaporative and floor cooling systems (Case 3), as shown in Figures 18 (a) and (b), was found to be uniformly distributed throughout the greenhouse, similar to Case 1, because there is no forced convection from the floor cooling system. Although the air movement in Case 3 is identical to Case 1, the average air velocity inside the greenhouse is higher, at 0.33 m/s.

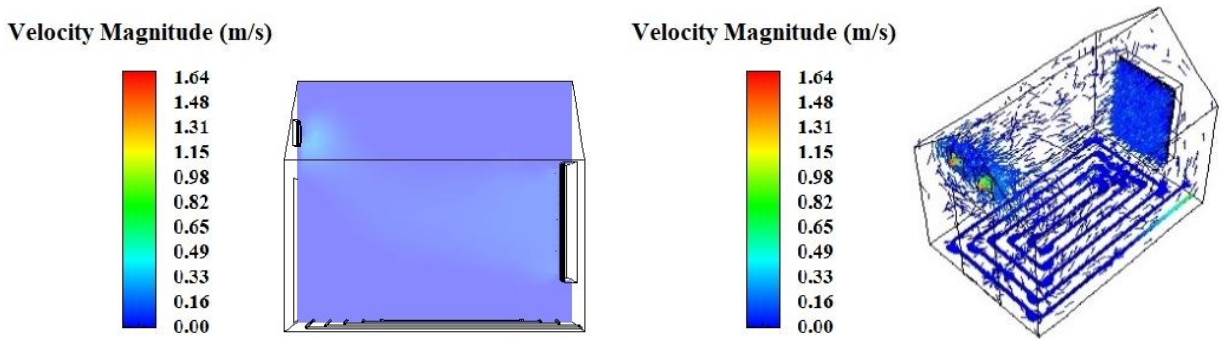

(a) (b)

Fig. 18. The velocity distribution at the greenhouse's walls and floor (case 3)

In case 3, the greenhouse had the evaporative and floor cooling system. The temperature of the floor cooling is 19 ºC. As shown in Figure 19, the minimum and maximum temperatures were 19 ºC and 34 ºC, respectively.

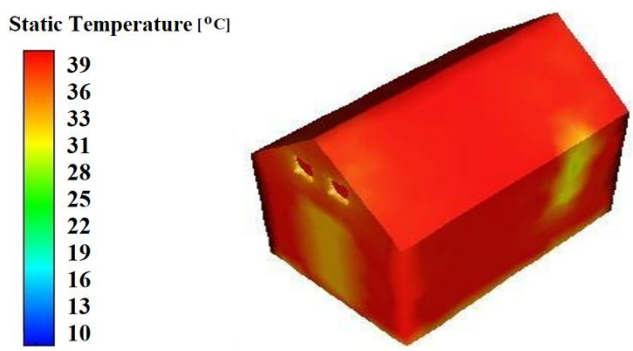

Fig. 19. The distribution of temperatures at the greenhouse's walls and floor (case 3)

Figures 20 (a) and (b) show the temperature distribution simulation results for the greenhouse which has a floor cooling system that works in conjunction with an evaporative cooling system. The average air temperature of the greenhouse for heights at 0.5, 1.0, 1.5 and 1.9 meters were 19 ºC, 25 ºC, 28 ºC and 33 ºC, respectively. As shown in Figures 20 (a) and (b), the average air temperature in the greenhouse was lower in Case 3 compared to Cases 1 and 2. This improvement is due to the combined effects of the floor and evaporative cooling system, which result in a natural convection phenomenon, with the most violent airflow movement occurring near the walls and ceiling.

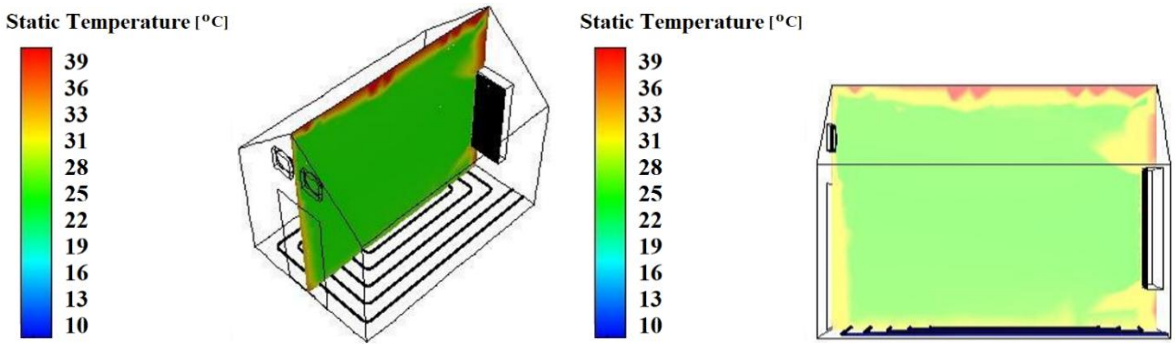

(a) (b)

Fig. 20. The temperature distribution contours at the height measurement (X-Y plane) of 0.5 to 1.9 meters (case 3)

4. Conclusion

Computational fluid dynamics (CFD) simulations were used in the study to examine temperature distribution in the effects of floor cooling on the greenhouse under different cooling systems, using the finite volume method and various turbulence models. Three scenarios were examined: Case 1, the greenhouse with only the evaporative cooling system; Case 2, the greenhouse with only the floor cooling system; and Case 3, the greenhouse equipped with the floor cooling system and the evaporative cooling system. The findings indicated that the Realizable of k-ε turbulence model provided superior accuracy compared to the Standard of k-ε model in simulating temperature distributions within the greenhouse. This is evident from the lower percentage of errors in temperature predictions, particularly in cases involving complex cooling systems. However, significant discrepancies remained near the wall surface of a greenhouse (0.5 and 3 meters above the wall) compared to the experimental results. To address these discrepancies and improve the accuracy of the numerical simulations, the researchers incorporated a radiation model alongside the Realizable of k-ε turbulence model. The inclusion of the radiation model in conjunction with the Realizable of k-ε turbulence model improved the accuracy of simulations, especially in capturing temperature effects near the wall surface of a greenhouse. The combined model reduced percentage errors and aligned more closely with experimental data, particularly near the wall surface of a greenhouse. This study highlights the importance of selecting appropriate turbulence models and incorporating additional factors like radiation to accurately simulate and optimize greenhouse cooling systems. The findings provide significant insights for designers and improving greenhouse cooling strategies to achieve better environmental control.

5. Acknowledgments

This research was supported in part by the Graduate Program Scholarship from The Graduate School, Kasetsart University. This research was also financially supported by Kasetsart University Research and Development Institute and Faculty of Science and Engineering, Kasetsart University, Chalermphrakiat Sakon Nakhon Province Campus, Thailand.

References

[1] Attar I, Naili N, Khalifa N, Hazami M, Lazaar M, Farhat A. Experimental study of an air conditioning system to control a greenhouse microclimate. Energy Convers Manage. 2014;79:543–553.

[2] Abu-Hamdeh NH, Almitani KH. Solar liquid desiccant regeneration and nanofluids in evaporative cooling for greenhouse food production in Saudi Arabia. Sol Energy. 2016;134:202–210.

[3] Wu X, Zhao J, Olesen BW, Fang L, Wang F. A new simplified model to calculate surface temperature and heat transfer of radiant floor heating and cooling systems. Energy Build. 2015;105:285–293.

[4] Srivastava P, Khan Y, Bhandari M, Mathur J, Pratap R. Calibrated simulation analysis for integration of evaporative cooling and radiant cooling system for different Indian climatic zones. J Build Eng. 2018;19:561–572.

[5] Zheng X, Han Y, Zhang H, Zheng W, Kong D. Numerical study on impact of non-heating surface temperature on the heat output of radiant floor heating system. Energy Build. 2017;155:198–206.
[6] Romaní J, Cabeza LF, de Gracia A. Development and experimental validation of a transient 2D numeric model for radiant walls. Renew Energy. 2018;115:859–870.
[7] Dong J, Zheng W, Song M, Chen Z, Jiang Y. Numerical simulation on heating performances of a radiant-convective heating terminal. J Build Eng. 2021;39:1–10.
[8] Mičko P, Kapjor A, Holubčík M, Hečko D. Experimental verification of CFD simulation when evaluating the operative temperature and mean radiation temperature for radiator heating and floor heating. Processes. 2021;9(6):1–11.
[9] Liu J, Su M, Kim MK, Song S. Developing simplified numerical calculation and BP neural network modeling for the cooling capacity in a radiant floor cooling system. J Asian Archit Build Eng. 2024;23(1):754–772.
[10] Flores-Velázquez J, De la Torre-Gea G, Rico-García E, López-Cruz IL, Rojano-Aguilar A. Advances in computational fluid dynamics applied to the greenhouse environment. Appl Comput Fluid Dyn. 2002.
[11] Nuyjanthuek T, Pramuanjaroenkij A. The performance comparison of the floor cooling system working in the closed greenhouse during daytime and nighttime [Master's thesis]. Kasetsart University; 2023.
[12] ANSYS Inc. ANSYS FLUENT theory guide (Release 16.1). Canonsburg (PA): ANSYS Inc; 2014.
[13] Menter FR. Two-equation eddy-viscosity turbulence models for engineering applications. AIAA J. 1994;32(8):1598–1605.
[14] Yuce BE, Pulat E. Forced, natural and mixed convection benchmark studies for indoor thermal environments. International Communications Heat Mass Transf. 2018;92:1–14.
[15] Boussinesq J. Essai sur la théorie des eaux courantes. Mém Acad Sci. 1877;23(1):1–680.
[16] Launder BE, Spalding DB. Lectures in Mathematical Models of Turbulence. UK: Academic Press; 1972.